JOURNAL OF EXPERIMENTAL AND THEORETICAL PHYSICS, 2024, Vol. 165, No. 5, pp. 680–692

INFLUENCE OF A UNIFORM ELECTRIC FIELD ON VORTEX-LIKE MAGNETIC STRUCTURES IN PERFORATED FILMS

© 2024 E. B. Magadeev*, R. M. Vakhitov**

Ufa University of Science and Technology, 450076, Ufa, Russia

** e-mail: magadeeveb@gmail.com*

*** e-mail: VakhitovRM@yahoo.com*

Received October 26, 2023

Revised December 27, 2023

Accepted December 28, 2023

Abstract. The manifestations of the flexomagnetoelectric effect in thin ferromagnetic films with uniaxial easy-plane anisotropy and artificially created perforations in the presence of an external electric field normal to the film plane are investigated. It is shown that the influence of inhomogeneous magnetoelectric interaction in this case leads to the transformation of magnetic structures, which is necessarily accompanied by the deviation of the magnetization vector from the sample plane. For cases where the deviation angles are small, explicit expressions describing the magnetization distribution are obtained. It is proven that the impact of an electric field of certain strength can lead to changes in the topology of the ground state of the system. A simplified model is considered, explaining the features of changes in structures of this type, as well as allowing to establish conditions for their implementation.

DOI: 10.31857/S004445102405e079

1. INTRODUCTION

Despite the fact that in recent years semiconductor electronics has practically displaced devices operating on magnetic principles, research in the field of magnetic materials design has not lost its relevance at all. Interest in this topic is due, in particular, to deep and comprehensive study of vortex-like objects (skyrmions, bimerons, cylindrical magnetic domains, etc. [1-5]), which are considered promising for creating new generation micro- and nanoelectronic devices [6-8] due to their nanoscale dimensions, topological protection, high mobility, etc. [3, 5, 6]. Nevertheless, a number of issues important for the practical application of such objects remain unresolved, not least concerning the stability and controllability of vortexlike structures [9], especially at room temperatures. Thus, in most works devoted to this subject (see, for example, [1]), the Dzyaloshinskii-Moriya interaction, which becomes significant only at low temperatures [10,11], is considered as the key factor ensuring the stability of the studied nano-objects. At the same time, in nanostructured films, it manifests itself already at room temperatures, however at such small scales (~ 1 nm), fluctuations will arise that disturb the delicate balance of interactions responsible for the stability of vortex-like inhomogeneities [9]. Moreover, the Dzyaloshinskii-Moriya interaction parameter is essentially a fixed characteristic of the material, which significantly limits the possibilities of controlling structures formed under the influence of this interaction. In this sense, a more attractive alternative is the inhomogeneous magnetoelectric interaction (IMEI) [12, 13], which at the phenomenological level of description is similar to the Dzyaloshinskii-Moriya interaction [1], but directly depends on the magnitude of the applied electric field and completely disappears in the absence of the field. The relatively low interest in IMEI until recently is apparently explained by the fact that the associated flexomagnetoelectric effect is observed in a rather narrow class of magnetic materials [14-16]; moreover, the nature of this phenomenon still remains a subject of discussion [17, 18]. Nevertheless, the possibility of effective domain structure control through IMEI has already received several experimental confirmations [14, 19], and theoretical studies indicate the applicability

of this approach also to the control of vortex-like nano-objects [20]. In this case, control efficiency should primarily be understood as energy efficiency, associated with lower energy costs for creating electric fields compared to magnetic fields [19].

In works [21-23], perforated ferromagnetic films with strong uniaxial "easy-plane" anisotropy were studied, and it was shown that in the region of two or more closely spaced holes in such a film, localization of topologically protected vortex-like objects is possible, which can be used for recording and storing information in a ternary number system (later in [24], an alternative method of recording information on multiply connected samples with easy-plane anisotropy was also proposed, however only in a binary system). To switch between inequivalent states of these objects, pulses of both magnetic [25] and, apparently, electric field can be used. The latter is indicated by the results of study [20] (as well as similar reasoning in work [26] regarding multiferroics, where the role of IMEI was played by "conventional" magnetoelectric interaction), which examined the influence of IMEI on magnetization distribution in a sample with one hole (obviously, such a model is also suitable for describing a sample with several holes whose sizes are small compared to the distance between them [23]), where the easy-plane anisotropy constant was assumed to be infinitely large, so that the magnetization vector could not leave the film plane. For this case, it was shown that the effect of the field of a charged filament passed through the hole leads to the formation of stable structures of various topologies, while a uniform electric field does not affect the magnetization distribution at all. It is clear, however, that the latter statement may prove invalid at finite values of the anisotropy constant, since the appearance of non-circular trajectories of the magnetization vector significantly complicates the nature of IMEI. This work is devoted to the study of phenomena associated with this.

2. BASIC EQUATIONS

Let us consider a thin ferromagnetic film h, containing a circular hole with radius R, and introduce a cylindrical coordinate system, (r, φ, z) as shown in Fig. 1 (axis z is normal to the film plane). We will describe the direction of the unit magnetization vector $\mathbf{m}$ using angles α and θ, the first of which determines the vector's $\mathbf{m}$ emergence from the film plane, and the second – the orientation of its projection on the plane, so that

$$\mathbf{m} = (-\sin(\theta - \phi)\cos\alpha, \cos(\theta - \phi)\cos\alpha, \sin\alpha). \quad (1)$$

Let the sample be in a uniform electric field with intensity $\mathbf{E} \parallel z$. Then, taking into account IMEI and uniaxial anisotropy of the "easy plane" type, whose axis is parallel to axis z, the total energy of the magnet can be represented as

$$W = \int_0^{2\pi}\int_R^{\infty} \Phi h r dr d\phi, \quad (2)$$

where the energy density Φ is determined as follows [13, 23]:

$$\Phi = A\left[(\nabla\alpha)^2 + \cos^2\alpha(\nabla\theta)^2\right] + K\sin^2\alpha + M_s^2\,\mathbf{E}(b_1\mathbf{m}\,\mathrm{div}\,\mathbf{m} + b_2\mathbf{m}\times\mathrm{rot}\,\mathbf{m}). \quad (3)$$

Here A — is the exchange parameter, K — is the absolute value of the anisotropy constant, M_s — is the saturation magnetization, and b_1 and b_2 — are IMEI constants. Note that expressions (2) and (3) do not explicitly include terms corresponding to the contribution of demagnetizing fields. This is because in thin films their influence is mostly reduced to the appearance of shape anisotropy [27], which, if necessary, can be accounted for by replacing the constant with its effective value $K + 2\pi M_s^2$. The in-plane components of demagnetizing fields only slightly distort the magnetization distribution [22], which does not change the pattern of observed phenomena even in cases where crystalline anisotropy is practically absent, and the presence of an easy plane is provided exclusively by shape anisotropy [28]. Substituting (1) into (3) and equating to zero the variational derivatives of functional (2) with respect to functions α and θ, we obtain the following Euler-Lagrange equations, which the energy minima of the system must satisfy [27]:

$$A\left[2\Delta\alpha + \sin 2\alpha(\nabla\theta)^2\right] - K\sin 2\alpha + \beta\cos^2\alpha\left[\sin(\theta-\phi)\frac{1}{r}\frac{\partial\theta}{\partial\phi} + \cos(\theta-\phi)\frac{\partial\theta}{\partial r}\right] = 0, \quad (4a)$$

$$A\left[2\Delta\theta - 4\,\mathrm{tg}\,\alpha\nabla\theta\nabla\alpha\right] - \beta\left[\sin(\theta-\phi)\frac{1}{r}\frac{\partial\alpha}{\partial\phi} + \cos(\theta-\phi)\frac{\partial\alpha}{\partial r}\right] = 0, \quad (4b)$$

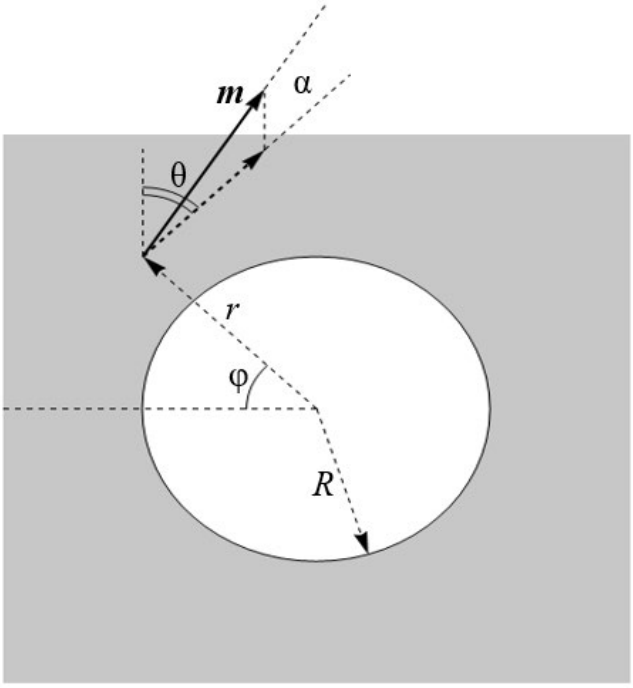

Fig. 1. Problem geometry

$$\beta = \beta_1 + \beta_2, \quad \beta_1 = b_1 M_s^2 E, \quad \beta_2 = b_2 M_s^2 E.$$

This system of equations must be supplemented with boundary conditions. First, at the hole boundary, the derivatives of energy density (3) with respect to $\partial\alpha / \partial r$ and $\partial\theta / \partial r$, must vanish, i.e., at $r = R$ we have

$$2A\frac{\partial\alpha}{\partial r} + (\beta_1 \sin^2\alpha + \beta_2 \cos^2\alpha)\sin(\theta - \phi) = 0, \quad (5a)$$

$$2A\frac{\partial\theta}{\partial r} - \beta_1 \operatorname{tg}\alpha \cos(\theta - \phi) = 0. \quad (5b)$$

Second, we will assume that at a large distance from the hole, the emergence of the magnetization vector from the film plane disappears, so that $\alpha(r \to \infty) = 0$. This condition allows excluding from consideration non-localized structures with quasi-periodic magnetization distribution [15], which, by analogy with chiral magnetics, could also form in samples of the studied type under the influence of fields **E** of sufficient magnitude.

Let's assume initially that there is no external field. Then $\beta = 0$, and the system of equations (4a), (4b) has a formal solution

$$\alpha = 0, \quad \theta = \theta_0 = k\phi + \phi_0, \quad (6)$$

where k — is an integer, and φ_0 — is an arbitrary constant. In [23], it was shown that solutions of type (6) correspond to energy minima (2) under the condition

$$K > A\left(\frac{c_{|k|}}{R}\right)^2, \quad (7)$$

where $c_0 = 0$, $c_1 = 0.320$, $c_2 = 1.066$, $c_3 = 1.902$ and so on. At the same time, the value k numbers topologically non-equivalent states of the magnet [21], which thus prove to be longlived even at $k \neq 0$, despite the fact that the global minimum of the system's energy is definitely achieved with a uniform magnetization distribution $k = 0$.

As a result of field activation **E** the magnetization distribution will no longer be described by relationships of type (6). Nevertheless, in cases where the angle α does not reach values $\pm\pi / 2$ at any point of the sample, the magnetic states can still be characterized by the value k, understanding it as the number of rotations made by the projection of vector **m** on the film plane during a complete clockwise circuit around the hole. However, it is certainly no longer correct to speak about topological non-equivalence of states with different values of k, and the stability conditions (7) become insufficient. Moreover, localized structures with a predetermined k may not exist at all at certain field strength values E. It is clear, however, that in most processes involving minor field changes **E**, the value k will be preserved, which makes it convenient to use in further analysis.

Note that solutions of type (6) at $k \neq 0$ correspond to magnetic structures that, generally speaking, are not isolated inhomogeneities. Nevertheless, in the presence of a second hole in the film, where the magnetic structure in the vicinity is characterized by the value $-k$, the magnetization distribution at a distance from both holes turns out to be uniform (more precisely, the values of the angle θ approach some limit according to the law r^{-1}, and the energy density Φ decreases according to the law r^{-4} [21]). The same is true for an arbitrary number of holes with a zero total value of k [22]. In this regard, the structures described by the system of equations (4a), (4b) should also be perceived as components of a larger isolated inhomogeneity, although for each of them separately, the limit $\theta(r \to \infty)$ may not exist. This, in particular, explains the absence of a condition for the angle θ similar to $\alpha(r \to \infty) = 0$.

3. STRONG ANISOTROPY APPROXIMATION

From the form of the system of equations (4a), (4b), it is clear that at $K \to \infty$ its solutions are expressed by relations (6) even in the presence of an external field ($\beta \neq 0$). Let the value K be finite but large, so that at least $K \gg A / R^2$, and condition (7) is satisfied with a significant margin. It is reasonable to assume that in this case the magnetization distribution in a nonzero field will be described by expressions close to (6), making it possible to use perturbation theory, representing angles α and θ as series in powers of a small parameter K^{-1} (since this parameter is not dimensionless, the exact meaning of its smallness requirement will be established later). Let $\theta = \theta_0 + \theta_1$, where $\theta_1 \sim \alpha \sim K^{-1}$. Then, keeping only non-small terms in equation (4a), we immediately obtain

$$\alpha = \frac{k\beta \sin[(k-1)\phi + \phi_0]}{2Kr}. \tag{8}$$

Note that this result seems to contradict the boundary condition (5a). In reality, its fulfillment will be ensured by rapid change of angle α in a small vicinity of the hole boundary, which has a width of order $\sqrt{A / K}$ and, accordingly, completely disappears within the framework of the studied approximation. For the same reason, based on formula (8), it would be incorrect to conclude about the absence of magnetization vector exit from the film plane at $k = 0$: it is easy to see that a uniform distribution of the form $\alpha = 0$, $\theta = \text{const}$ actually cannot satisfy condition (5a) at $\beta_2 \neq 0$. Nevertheless, in the presence of strong anisotropy, the scales of the forming inhomogeneity turn out to be vanishingly small.

The expression for energy density (3) up to terms of order K^{-1}, generally speaking, contains a term dependent on θ_1. Being proportional to $\partial\theta_1 / \partial\phi$, this term, however, gives zero contribution to integral (2), therefore it is expedient to introduce the quantity Φ, averaged over angles φ from 0 to 2π. Taking into account formula (8), this quantity, regardless of the function form θ_1 equals

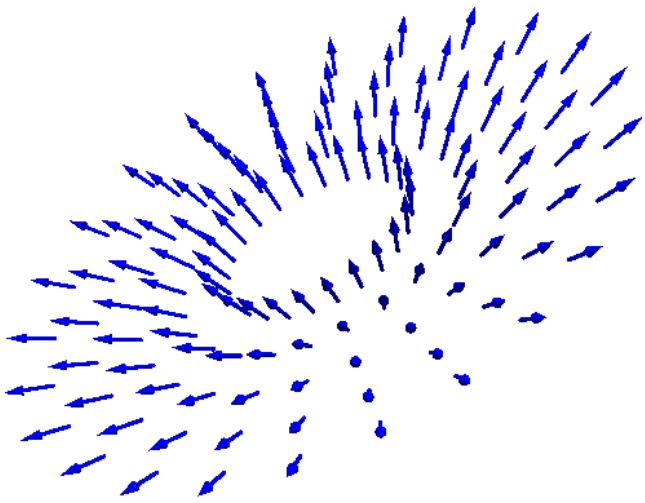

Fig. 2. Schematic representation of magnetization vector directions at different points of the sample in case of $k = 1$ in non-zero external field

$$\langle\Phi\rangle = \begin{cases} \dfrac{k^2 A}{r^2}\left(1 - \dfrac{\beta^2}{8AK}\right), & k \neq 1, \\ \dfrac{A}{r^2}\left(1 - \dfrac{\beta^2 \sin^2\phi_0}{4AK}\right), & k = 1. \end{cases} \tag{9}$$

From this relation it follows that at $k = 1$ the degeneracy with respect to angle φ_0 is removed by fields of arbitrarily small magnitude E. In this case, structures with $\phi_0 = \pm\pi / 2$, become stable, which corresponds to the radial direction of the **m** vector projection onto the sample plane (see Fig.2). At the same time, the distribution $\alpha = 0, \theta = \phi$, which at arbitrary values of parameters K and β formally satisfies both equations (4a), (4b), and conditions (5a), (5b), is not realized at $\beta \neq 0$, since $\phi_0 = 0$ does not minimize the energy density (9), but maximizes it.

Substituting (8) into equation (4b), accurate to terms of order K^{-1} we have

$$\Delta\theta_1 = \frac{k(k-2)\beta^2 \sin 2[(k-1)\phi + \phi_0]}{8AKr^2}. \tag{10}$$

In the same approximation, condition (5b) at the boundary $r = R$ takes the form

$$\frac{\partial\theta_1}{\partial r} = \frac{k\beta\beta_1 \sin 2[(k-1)\phi + \phi_0]}{8AK\,R}. \tag{11}$$

At $k = 1$ the right-hand sides of expressions (10) and (11), considering $\phi_0 = \pm\pi / 2$ become zero, due to

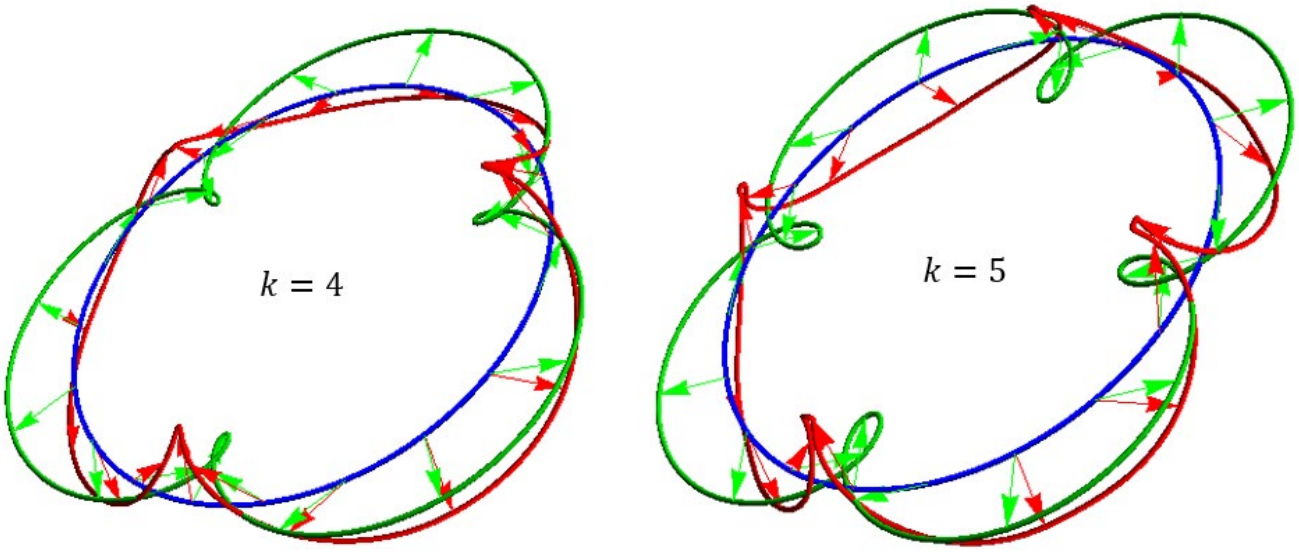

Fig. 3. Schematic representation of magnetization distribution depending on the angle φ при двух at two different values of k. The blue color shows the circle r = const, at whose points the magnetization directions are considered. The green color shows the positions of the magnetization vector ends when there is no electric field and the magnetization vector does not leave the film plane, while red shows the case when the field is on. Green and red arrows illustrate the direction of the magnetization vector at individual points of the circle for both cases

which $\theta_1 = 0$. From here, summarizing formulas (6), (8), and (9), we obtain

$$\alpha = \pm\frac{\beta}{2Kr}, \quad \theta = \phi \pm \frac{\pi}{2}, \quad \langle\Phi\rangle = \frac{A}{r^2}\left(1 - \frac{\beta^2}{4AK}\right). \quad (12)$$

At $k \neq 1$ the bounded solution of equation (10), satisfying condition (11), looks as follows:

$$\theta_1 = -\frac{k\beta \sin 2[(k-1)\phi + \phi_0]}{32(k-1)^2 AK} \times \times\left[(k-2)\beta + 2\,|\,k-1\,|\beta_1\left(\frac{R}{r}\right)^{2|k-1|}\right]. \quad (13)$$

From formulas (8) and (13), it follows that switching on the field **E** does not change the symmetry of the magnetic structure of type (6), which consists in the existence of a rotational axis of order $|\,k-1\,|$ (see Fig. 3). However, the magnetization distribution turns out to be different from (6) even at a large distance $r \gg R$ from the hole. Indeed, correction (13), unlike angle (8), has at $r \to \infty$ a non-zero limit, meaning that in the entire volume of the sample, except for a small neighborhood of the hole, the magnetization vector will rotate by some angle while practically remaining in the plane. The exception is the structure corresponding to $k = 2$, in which case correction (13) with increasing still decreases to zero according to the law r^{-2}. This circumstance is a particular consequence of the fact that the limit $|\,\theta_1\,|$ at $r \to \infty$, as can be easily verified, is determined by the value $|\,k-1\,|$. Thus, for $k = 2$ this limit must be exactly the same as for $k = 0$.

Note that fulfilling the above condition $K \gg A / R^2$ does not yet guarantee the correctness of the considered approximation, since this condition establishes a relationship only between anisotropy and exchange interaction, but does not affect IMEI. As a result, the value β (for simplicity, we will consider β_1 and β to be of the same order) may turn out to be so large that corrections (8) and (13) will no longer have the character of perturbations. Their smallness is ensured by the additional condition $K \gg \beta^2 / A$, which should be checked along with $K \gg A / R^2$. Note that at $|\,\beta\,| \approx A / R$ these conditions become equivalent.

4. WEAK FIELD APPROXIMATION

Within the framework of the strong anisotropy approximation considered above, the possibility of applying perturbation theory was ensured by the fact that vector **m** cannot significantly deviate from the pronounced easy plane even at substantial values of the applied field E. However, if we limit

ourselves to considering weak fields, then the resulting magnetization distribution under their influence should be close to distribution (6) even at moderate values of constant K, satisfying condition (7). In this case, the quantities β and β_2 (quantitative conditions of their smallness will be established later), proportional to the intensity E play the role of small parameters. Assuming $\theta_1 \sim \alpha \sim \beta \sim \beta_2$, instead of equation (4a) with accuracy up to terms of order β we have

$$\Delta\alpha + \left(\frac{k^2}{r^2} - \frac{K}{A}\right)\alpha = -\frac{k\beta\sin[(k-1)\phi + \phi_0]}{2Ar}, \quad (14)$$

and instead of the boundary condition (5a) at $r = R$

$$\frac{\partial\alpha}{\partial r} = -\frac{\beta_2\sin[(k-1)\phi + \phi_0]}{2A}. \quad (15)$$

With the same accuracy from (4b) we obtain the Laplace equation $\Delta\theta_1 = 0$, and from (5b) – the condition for the derivative $\partial\theta / \partial r$ to be zero at the hole boundary. Thus, within the framework of the considered approximation $\theta_1 \equiv 0$, i.e., the correction θ_1, as in the case of relation (13), is proportional to β^2.

From the form of expressions (14) and (15), it follows that

$$\alpha = \tilde{\alpha}(r)\sin[(k-1)\phi + \phi_0],$$

where $\tilde{a}(r)$ thus describes the radial dependence of the angle $\alpha(r, \phi)$ and represents a bounded solution at $r \to \infty$ of the equation

$$\begin{aligned}&\tilde{\alpha}'' + \frac{1}{r}\tilde{\alpha}' + \left(\frac{2k-1}{r^2} - \frac{K}{A}\right)\tilde{\alpha} = -\frac{k\beta}{2Ar},\\ &\tilde{\alpha}'(R) = -\frac{\beta_2}{2A}.\end{aligned} \quad (16)$$

Obviously, at $k \neq 1$ the value φ_0 can be arbitrary. At $k = 1$ expression (2), accurate to terms of order β^2 can be represented as

$$W = W^{(0)} + \sin^2\phi_0 W^{(1)},$$

where $W^{(0)}$ depends neither on φ_0, nor on $\tilde{\alpha}(r)$, and $W^{(1)}$ is a functional of the function $\tilde{\alpha}(r)$. Meanwhile, the functional $W^{(1)}$ becomes zero at $\tilde{\alpha} \equiv 0$, but this function does not satisfy the condition of its extremum. Consequently, $W^{(1)}$ can certainly take negative values, and the minimum energy W, as in the case of strong anisotropy approximation, is achieved at $\phi_0 = \pm\pi / 2$, when $\alpha = \pm\tilde{\alpha}(r)$ (see Fig. 2).

Let's introduce the following function, which is a solution to equation (16) at $\beta = 0$, $\beta_2 = \sqrt{AK}$:

$$F(r) = \frac{Q_{\sqrt{1-2k}}\left(\sqrt{\frac{K}{A}}r\right)}{Q_{-1+\sqrt{1-2k}}\left(\sqrt{\frac{K}{A}}R\right) + Q_{1+\sqrt{1-2k}}\left(\sqrt{\frac{K}{A}}R\right)}, \quad (17)$$

where Q — is the modified Bessel function of the second kind (the more conventional notation K for this function is not used here to avoid confusion with the previously introduced notation for the anisotropy constant). Then, due to the linearity of equation (16), its solution in the general case has the following form:

$$\tilde{\alpha}(r) = \frac{\beta_2}{\sqrt{AK}}F(r) + \frac{\beta}{\sqrt{AK}}\left[\tilde{\alpha}_0(r) + 2\sqrt{\frac{A}{K}}\,\tilde{\alpha}_0'(R)\,F(r)\right], \quad (18)$$

where $\tilde{\alpha}_0(r)$ — is a particular solution of (16) at $\beta = \sqrt{AK}$ and arbitrary value β_2.

The first term on the right side of expression (18) is due to the influence of IMEI at the hole boundary and rapidly decreases with increasing r. Nevertheless, its contribution becomes dominant if $\beta = 0\,(b_1 = -b_2)$ or $k = 0$ (resulting in $\tilde{\alpha} \equiv 0$). Moreover, due to the presence of this term at $\beta_2 \neq 0$ the magnetization vector's emergence from the film plane will be observed at arbitrary values of k, including $k = 0$, i.e., even a uniform magnetization distribution will be distorted as a result of the **E** field inclusion. Notably, this edge effect does not disappear even when the strong anisotropy condition is met $K \gg A / R^2$. Indeed, in this case, the value of $F(R)$, according to (17), tends to the limit $1 / 2$, meaning that the angle α should reach the value $\beta_2 / 2\sqrt{AK}$, at the hole boundary, which generally significantly exceeds the angles of deviation from the plane determined by formula (8). Nevertheless, the exponential decay nature of function (17) leads to the fact that already at a distance of several $\sqrt{A / K} \ll R$ from the hole boundary, the influence

of the edge effect becomes imperceptible, and the values of angle α sharply decrease.

The asymptotic behavior of solution (18) at $r \to \infty$ is determined by the form of the particular solution $\tilde{\alpha}_0(r)$. At the same time, from equation (14), it can be concluded that even at moderate values of K the asymptotic behavior of angle α at a large distance from the hole is described by relation (8). This allows us to set

$$\tilde{\alpha}_0 \approx \frac{k}{2r}\sqrt{\frac{A}{K}},$$

from which instead of (18) we have the following approximate solution of equation (16):

$$\tilde{\alpha}(r) = \frac{\beta_2}{\sqrt{AK}}F(r) + \frac{k\beta}{2Kr} - \frac{k\beta}{R^2}\sqrt{\frac{A}{K^3}}F(r). \quad (19)$$

Figure 4 shows the graphs of dependence $\tilde{\alpha}(r)$, obtained as a result of numerical solution of equation (16) at $\beta_1 = \beta_2, k = \pm 1$ and various values of K, as well as graphs of function (19) at the same parameter values. It is easy to see that the approximate expression (19) reflects the behavioral features of function $\tilde{\alpha}(r)$ quite correctly, and the accuracy of approximation, as expected, increases with the growth of value K. In particular, in the case of $k = 1$ the maximum relative error, which is achieved at $r \approx 1.4R$, is 13% at $KR^2 / A = 5$, but already at $KR^2 / A = 20$ becomes less than 4%. It should be noted that at values of ratio $KR^2 / A \geqslant 20$ not only formula (19) but also relation 4% has accuracy no worse than $F(R) \approx 1/2$. This allows us to write the following approximate expression for the values of angle α, reached at the hole boundary:

$$\alpha_m = \tilde{\alpha}(R) = \frac{\beta_2}{2\sqrt{AK}} + \frac{k\beta}{2KR} - \frac{k\beta}{2R^2}\sqrt{\frac{A}{K^3}}. \quad (20)$$

Despite the fact that relation (20), which represents the sum of the first three terms of expansion α_m in powers of $K^{-1/2}$, becomes valid at rather large values of K, it, of course, could not have been obtained within the strong anisotropy approximation. We should also emphasize that the value α_m cannot be identified with the maximum angle of magnetization vector exit from the sample plane: for example, from Fig. 4 it follows that in the case of $k = -1$, $KR^2 / A = 5$ (solid blue curve in the lower graph) the values of $|\tilde{\alpha}|$ at $r \approx 2R$ exceed α_m by more

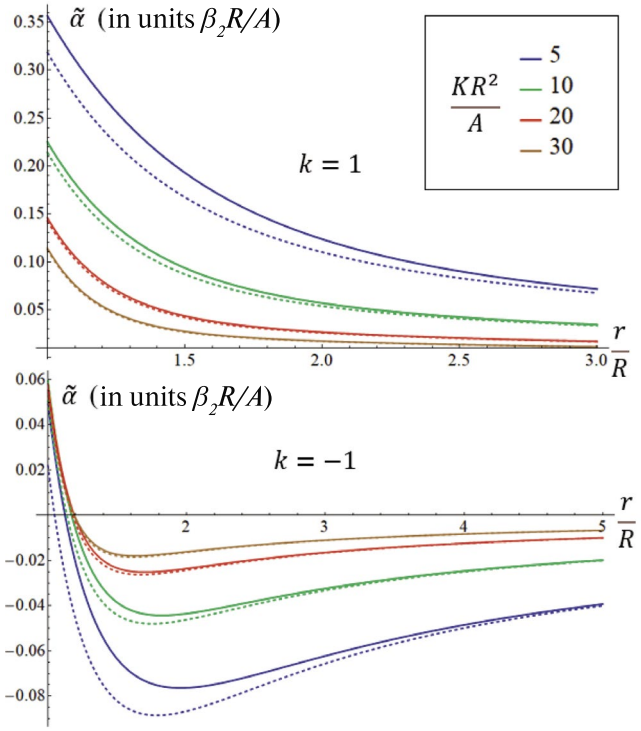

Fig. 4. Graphs of the radial part $\tilde{\alpha}(r)$ dependence $\alpha(r,\phi)$ of the magnetization vector deviation angle from the film plane at $\beta_1 = \beta_2$ (or, equivalently, when the NMMI constants b_1 and b_2, which are proportional to the values β_1 and β_2, are equal), $k = \pm 1$ and different values of the absolute magnitude of the anisotropy constant K. Values $\tilde{\alpha}$ are given in units of the dimensionless quantity $\beta_2 R / A$. Solid lines – values $\tilde{\alpha}$, obtained numerically; dashed lines – result of using the approximate expression

than 50% (in particular, directly at $r = 2R$ we have $|\tilde{\alpha}| \approx 1.55\alpha_m$, since $\tilde{\alpha}(R) \approx 0.049\beta_2 R / A$, $\tilde{\alpha}(2R) \approx -0.076\beta_2 R / A$). Nevertheless, due to its simplicity, relation (20) may prove to be very convenient both for estimating the degree of distortion of structures like (6) under the influence of an electric field and for experimental verification of the theory developed here..

From formula (18), it follows that the weak field approximation is applicable only under the condition $|\beta| \ll \sqrt{AK}$. The fulfillment of this condition together with inequality (7) ensures the smallness of each of the three terms in the right-hand side of formula (20), which eliminates the need to impose any additional restrictions. In particular, the condition $|\beta| \ll A / R$, which could correspond to the smallness of the DMI influence compared to the exchange interaction, is actually redundant; furthermore, it was not used in any way when transitioning from (4a) to equation (14). Thus, the applicability domain of the weak field

approximation completely contains the applicability domain of the strong anisotropy approximation ($K \gg \beta^2 / A, K \gg A / R^2$), which could serve as an argument for abandoning the use of the latter. It is clear, however, that within the weak field approximation, relations like (9) and (13) can no longer be obtained in a transparent form due to the more complex dependence of α on r compared to (8). This explains the importance of both considered approximations.

5. CASE $k = 1$

From formulas (9) and (12), valid for large values of K, it follows that the inclusion of an external electric field leads to a decrease in energy by the same factor for all states of the system, except for $k = 1$. At $\beta \ll \sqrt{AK}$ the only consequence of this effect is the removal of degeneracy by the sign of the value k at $k = \pm 1$, while the rest of the energy spectrum of the system remains unchanged. With increasing value of β the angle values θ at $k \neq 1$, according to formula (13), begin to change significantly throughout the sample volume, due to which relation (9) can no longer be used for quantitative estimates. Nevertheless, it allows to qualitatively trace the following important trend: if the value of β is large enough that at some $k \neq 1$ the system energy becomes negative, then states with $k \to \pm\infty$. formally become energetically favorable. Physically, this corresponds to the stabilization of non-localized quasiperiodic structures [15]), which are not considered in this work. Thus, isolated inhomogeneities with $k \neq 1$ cannot represent the ground state of the system. However, we will show that regarding the case of $k = 1$ this statement is incorrect.

Note that the system of equations (4a), (4b) with boundary conditions (5a), (5b) can have two classes of solutions for which $\theta = \phi + \phi_0$. First, $\alpha = 0, \theta = \phi$, which, as mentioned above, generally does not correspond to the minimum energy (2). Second, $\theta = \phi \pm \pi / 2$ (see Fig. 2), while the angle α, which in this case depends only on the distance r to the center of the hole, must be determined from equation (4a), which takes the form

$$\alpha'' + \frac{1}{r}\alpha' + \left(\frac{1}{r^2} - \frac{K}{A}\right)\sin\alpha\cos\alpha = \mp\frac{\beta}{2Ar}\cos^2\alpha. \quad (21)$$

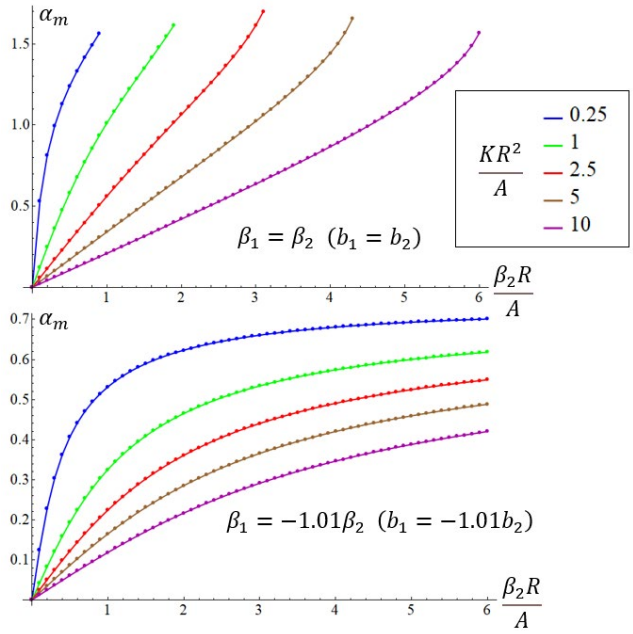

Fig. 5. Values of angle α_m of magnetization vector deviation from the film plane at the hole boundary depending on the value of β_2, proportional to external field strength, in case $k = 1$ (typical magnetization distribution for this case is shown in Fig. 2) at different values of absolute anisotropy constant K. Upper and lower graphs differ in the ratio between values β_1 and β_2 (or, equivalently, between the values of NMIE constants b_1 and b_2, to which the values β_1 and β_2 are proportional)

Also, due to (5a), we obtain the following boundary condition at $r = R$:

$$\alpha' = \mp\frac{\beta_1 \sin^2\alpha + \beta_2 \cos^2\alpha}{2A}. \quad (22)$$

Since at a large distance from the hole boundaries, the relation $|\alpha| \ll 1$, must hold, from (21) we conclude that the asymptotic behavior of the function $\alpha(r)$ at $r \to \infty$ is described by formula (12). Obviously, in this case, the averaged energy density $\langle\Phi\rangle$ far from the hole must also be described by formula (12). The integral (2) turns out to be divergent, therefore, the region of large r will give the determining contribution to the system energy W, and the sign of the energy will depend on the sign of the coefficient in expression (12) for $\langle\Phi\rangle$: if

$$|\beta| > 2\sqrt{AK}, \quad (23)$$

then $W \to -\infty$, so that the state with $k = 1$ becomes energetically favorable compared to $k = 0$ (we emphasize that at $k = 0$ the finite value W is also negative due to the influence of edge effects).

However, the question of the very existence of a solution to equation (21) under boundary condition (22) remains open.

Fig. 5 shows the graphs of angle $\alpha_m = \alpha(R)$ dependency at the hole boundary on the value of β_2 at different values of K for cases $\beta_1 = \beta_2$ and $\beta_1 = -1.01\beta_2$. These dependencies were obtained through numerical minimization of energy (2) with respect to function $\alpha(r)$ considering equality $\theta = \phi + \pi/2$, although numerical solution of equation (21) under condition (22) leads to the same results (in practice, the choice in favor of minimization algorithm was determined by its ability to obtain magnetization distribution even in cases when solutions of corresponding Euler-Lagrange equations formally do not exist). The presented graphs show that under condition $\beta_1 = -1.01\beta_2$ structures of the studied type are observed at arbitrary values of β_2, and at $\beta_2 \to \infty$ the values of α_m reach some limit less than $\pi/2$. Thus, for any predefined value of constant K such a large electric field strength E, can be selected that condition $|\beta| = 0.01\beta_2 > 2\sqrt{AK}$ will be satisfied, and the state with $k = 1$ will become fundamental for the system (it was to demonstrate this circumstance that example $\beta_1 = -1.01\beta_2$ was considered instead of the similar example $\beta_1 = -\beta_2$, where dependencies in Fig. 5 remain practically the same, but $\beta \equiv 0$). Conversely, in case $\beta_1 = \beta_2$ angle α_m approaches $\pi/2$ at some finite values of β_{2m} of value β_2, depending on constant K (for example, at $KR^2/A = 2.5$ we have $\beta_{2m}R/A \approx 3.1$), and at $\beta_2 > \beta_{2m}$ the forming magnetization distribution no longer has the character of an isolated inhomogeneity. Calculations for values KR^2/A in the range from 0.25 to 10 with a step of 0.25 allow obtaining the following empirical relation, which is satisfied with accuracy not worse than 5%:

$$\beta_{2m} = 2\sqrt{AK}. \tag{24}$$

Accordingly, the state with $k = 1$ becomes fundamental for the system if condition

$$\sqrt{AK} < \beta_2 < 2\sqrt{AK},$$

is met, i.e., field strength E must take values from a known interval.

A significant part of the observations described above, including relation (24), is difficult to explain based on the analysis of expressions (21) and (22) without additional assumptions. Nevertheless, they receive a clear interpretation within the framework of a simplified model, which is discussed below.

6. MODEL OF A STRAIGHT BOUNDARY

From the analysis conducted above, it is clear that the possibility of existence of structures corresponding to the value $k = 1$, is determined mainly by the feasibility of boundary conditions of type (22). To study this question in more detail, note that in the vicinity of the hole boundary, the presence of curvature of this boundary should practically not affect the magnetization distribution. Therefore, instead of a sample containing a circular hole (see Fig. 1), we can consider an approximate model in which the hole boundary is straight, i.e., the magnet fills a half-plane. Mathematically, this corresponds to the limiting transition $R \to \infty$, where the finite value $x = r - R$ plays the role of a Cartesian coordinate in this case. Thus, instead of (21), we obtain the following equation:

$$\alpha'' = \frac{K}{A}\sin\alpha\cos\alpha. \tag{25}$$

While the form of the boundary condition (22), which must be satisfied at $x = 0$, remains unchanged.

Equation (25) has the following integral:

$$\alpha'^2 - \frac{K}{A}\sin^2\alpha = \text{const}. \tag{26}$$

For a positive value of the constant in the right-hand side of relation (26), the value $|\alpha|$ will grow indefinitely at $x \to \infty$, which corresponds to the formation of a non-localized structure with a quasi-periodic distribution of magnetization. For a negative value of the constant, relation (26) describes oscillations of the angle α around the position $\pi/2$, which in the presence of "easy-plane" type anisotropy cannot correspond to the energy minimum. Therefore, in the case of an isolated magnetic inhomogeneity, the discussed constant must be equal to zero, from which, taking into account condition (22), we have (the "minus" sign before the second term does not affect further reasoning and is chosen here for definiteness):

$$(\beta_1 - \beta_2)\sin^2\alpha_m - 2\sqrt{AK}\sin\alpha_m + \beta_2 = 0. \tag{27}$$

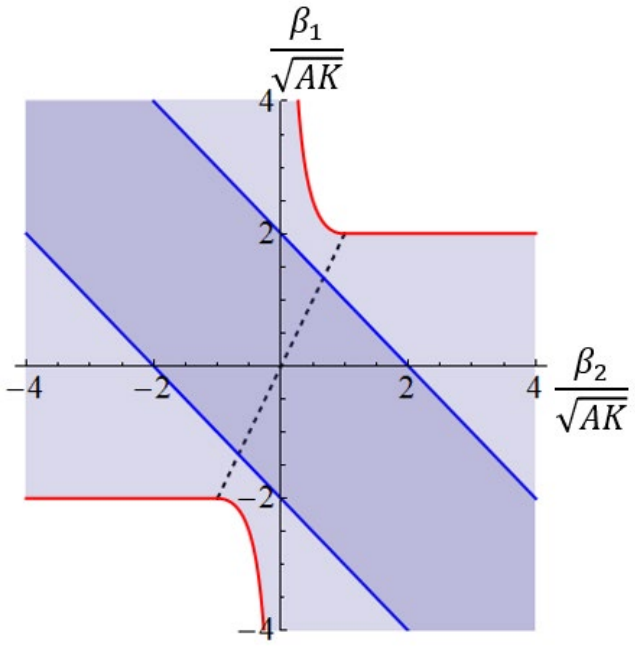

Fig. 6. Diagram of parameter values β_1 and β_2 (proportional to NMEE constants b_1 and b_1 respectively, as well as electric field intensity E), at which magnetic structures corresponding to $k = 1$, exist (dark gray area), or exist and represent the ground state of the system (light gray areas). Red and blue lines show the boundaries of the regions. The dashed line corresponds to equality $\beta_1 = 2\beta_2$

Equation (27) is generally quadratic with respect to $\sin\alpha_m$, and the existence of at least one root not exceeding 1 in absolute value is a condition for the existence of a magnetic structure with $k = 1$. In particular, in the degenerate case $\beta_1 = \beta_2$ the single root of equation (27) is determined by the relation

$$\sin\alpha_m = \beta_2 / (2\sqrt{AK}).$$

Consequently, $|\beta_2| < 2\sqrt{AK}$, which fully agrees with the empirical formula (24). Moreover, when the value β_2 reaches its critical value, the angle α_m becomes equal to $\pm\pi/2$, which also corresponds to the pattern observed in Fig. 5.

The diagram in Fig. 6 shows combinations of values β_1 and β_2 (recall that $\beta_1 = b_1 M_s^2 E$, $\beta_2 = b_2 M_s^2 E$), at which the above requirements for equation (27) are met (these combinations correspond to all points lying between the two red curves). It is easy to see that depending on the relationship between the NMEE constants b_1 and b_2 there are three different scenarios for the modification of magnetic inhomogeneity with increasing intensity E of the electric field (which causes proportional growth of β_1 and β_2). First, if these constants are values of different signs $b_1/b_2 < 0$), then even at $E \to \infty$ the magnetic inhomogeneity remains solitary. In this case, the value of angle α at the sample boundary, according to (27), tends to the limit

$$|\alpha_m| = \operatorname{arcctg}\sqrt{-b_1 / b_2}.$$

In the case of $b_1 \approx -b_2$ we have $|\alpha_m| \approx \pi/4$, which agrees well with the position of the asymptote of the corresponding graphs in Fig. 5. Second, if $0 < b_1 / b_2 < 2$, then when the value $|\beta_1|$ reaches $2\sqrt{AK}$ the angle α_m becomes equal to $\pm\pi/2$ and further increase in intensity E while maintaining the inhomogeneity structure becomes impossible. Third, if $b_1 / b_2 > 2$, then the maximum value of E, at which a solitary inhomogeneity can still exist, is determined by the relation

$$\beta_1 = \beta_2 + AK / \beta_2.$$

At this value of E both roots of the quadratic equation (27) become equal to

$$\sin\alpha_m = \beta_2 / \sqrt{AK},$$

while with further intensity increase, these roots become complex.

Summarizing the above, we note that the value of angle α_m, which is achieved at the maximum allowable intensity E, in all cases can be expressed only through the ratio of NMEW constants b_1/b_2:

$$|\alpha_m| = \begin{cases} \operatorname{arcctg}\sqrt{-b_1 / b_2}, & b_1 / b_2 < 0, \\ \pi/2, & 0 < b_1 / b_2 < 2, \\ \operatorname{arcctg}\sqrt{b_1 / b_2 - 2}, & b_1 / b_2 > 2. \end{cases} \quad (28)$$

We also present an explicit expression for the values E, at which structures of the studied type can exist:

$$E < E_{max} = \begin{cases} \infty, & b_1 / b_2 < 0, \\ \dfrac{2\sqrt{AK}}{M_s^2 |b_1|}, & 0 < b_1 / b_2 < 2, \\ \dfrac{\sqrt{AK}}{M_s^2 \sqrt{b_2 (b_1 - b_2)}}, & b_1 / b_2 > 2. \end{cases} \quad (29)$$

A similar condition (23), under which the state with $k = 1$ becomes energetically favorable, can be written as follows:

$$| E | < E_{min} = \frac{2\sqrt{AK}}{M_s^2 | b_1 + b_2 |}. \qquad (30)$$

Thus, if the material parameters of the magnet are known, formulas (29) and (30) allow calculating the range of intensity values E, at which the ground state of the system corresponds to the magnetization distribution similar to that shown in Fig. 2. These values correspond to points belonging to the light gray areas in Fig. 6 (blue lines on the diagram show the boundaries $| E | = E_{min}$, and red lines show $| E | = E_{max}$). From this, it can be seen that the discussed ranges exist at arbitrary values of the ratio $b_1 / b_2 \neq -1$, however, at $b_1 / b_2 \approx 2$ they become quite narrow.

It is necessary to separately address the fact that the radius of the hole R does not explicitly appear in either formula (29) or (30). From this, one might incorrectly conclude that the obtained results remain fully valid even at $R = 0$, i.e., in the absence of a hole. It is clear, however, that at $R \ll \sqrt{A / K}$ the limiting transition $R \to \infty$, which underlies the derivation of relation (29), loses its meaning. Nevertheless, the formation of structures corresponding to $k = 1$, is fundamentally possible in films without perforations. Indeed, in the case of a sample with such geometry, equation (21) can also have a non-trivial solution, which instead of (22) will satisfy a condition of the form $\alpha(r = 0) = \pm\pi / 2$. The asymptotic behavior of this solution at $r \to \infty$, as in the presence of a hole, will be determined by relations (12), and therefore, condition (30) remains valid, under which the inhomogeneity becomes energetically favorable. This essentially implies that the appearance of vortex-like inhomogeneities is not directly related to the presence of perforations: when a field of sufficient strength is applied, similar structures can equally arise both in the hole region and far from it (the similarity of structures of these two types is further enhanced by the fact that, according to formula (28), the value of angle α at the hole boundary can also in some cases approach $\pm\pi / 2$). Note, however, that in the absence of a hole (or far from it), the nucleation of inhomogeneous structures is always associated with spontaneous breaking of the system's translational symmetry, therefore the localization of a vortex-like structure in the hole region is generally much more likely. In this sense, perforations should be considered as distinctive crystallization centers artificially introduced into the system; it is reasonable to expect that in their presence, fluctuation mechanisms of inhomogeneous structure formation outside the holes should be either significantly weakened or completely suppressed. Another significant disadvantage of vortexlike inhomogeneities forming outside the holes is that during slow removal of the external field, they do not transition to a state of type (6) while preserving the value of $k = 1$, but simply collapse. This explains the low interest in structures of this type within the framework of the present study.

7. CONCLUSION

Despite the purely theoretical nature of this work, the results obtained allow for potentially solving a number of important practical tasks related to the control of inhomogeneous magnetic structures. First, the fact that under the influence of a uniform electric field, the magnetization vector begins to deviate from the film plane can be used to identify the current state of the system. Indeed, the calculations show that the spatial distribution of the normal component of the magnetization vector, which appears when the field is switched on, depends not only on the value of k, which determines the topology of the vortex-like structure, but also on the orientation of the structure in the plane. Moreover, the value of k be determined by the maximum angle α_m of the magnetization vector deviation at the hole boundary: the relationship between these quantities is practically linear. Since the influence of NMEE does not change the symmetry of magnetic structures, after the electric field pulse ends, they will relax into a state that completely coincides with the initial one, which ensures high reliability of the described approach to identifying the system state.

Secondly, the provided estimates of magnetic structure distortion by the electric field allow us to judge the characteristic magnitude of field strength at which the flexomagnetoelectric effect becomes noticeable. Thanks to this, in particular, it becomes possible to select such materials in which the control of vortex-like structures by means of an electric field

is not associated with excessive energy consumption, while sensitivity to parasitic external fields remains low.

Third, the change in the topology of the ground state of the magnetic structure in fields of certain magnitude opens up possibilities for implementing the following scenario. Let's assume that initially the magnetization distribution is close to uniform, corresponding to the value $k = 0$. As a result of rapid field application, the system will transition to a new ground state with $k = 1$. If after this the field strength is gradually reduced to zero, the system may remain in a state with $k = 1$, which will already be metastable, but long-lived due to topological reasons [21]. Such possibility of switching the system state through pulse exposure indicates the prospects of using perforated films as a basis for creating rewritable memory. Note that in practice, pairs of closely spaced holes should be used to solve this problem [21]: only in this case the forming magnetic inhomogeneities become well localized in space. Moreover, there is no need to directly affect both holes in the pair simultaneously: as the analysis of a similar scenario for the case of magnetic field control shows [25], when one of the structures is transferred from a state with $k = 0$ to a state with $k = 1$ the second structure associated with it spontaneously transitions to a state with $k = -1$ under the influence of exchange interaction. This becomes particularly important due to the fact that, unlike the electric field of a charged filament, which allows stabilizing structures with arbitrary value of k [20], a uniform electric field can only stabilize the state with $k = 1$, but not with $k = -1$. Such lack of control flexibility, however, should be fully compensated by the relative simplicity of creating uniform fields.

Despite the attractiveness of the approaches described above, it must be acknowledged that their practical implementation may prove quite difficult. The localization of vortex-like structures of the studied type on nanoscale perforations is only possible in materials with exceptionally strong easy-plane anisotropy (for example, $NdCo_5$ [23]), in which the flexomagnetoelectric effect is generally not observed. A solution to this situation could be either artificial creation of the required anisotropy, for example in garnet ferrite films, or nanostructuring of magnetic uniaxial films to enhance NMEW. Either way, this challenge may prove quite serious for modern materials science.

FUNDING

The work was carried out within the framework of the state assignment for scientific research laboratories (order MN-8/1356 dated 20.09.2021)

REFERENCES

1. A. Bogdanov and A. Hubert, J. Magn. Magn. Mater. 138, 255 (1994).
2. T. Shinjo, T. Okuno, R. Hassdorf et al., Science 289, 930 (2000).
3. K. Y. Guslienko, J. Nanosci. Nanotechnol. 8, 2745 (2008).
4. S. Mühlbauer, B. Binz, F. Jonietz et al., Science 323, 915 (2009).
5. A. N. Bogdanov and C. Panagopoulos, Nat.Rev. Phys. 2, 492 (2020).
6. K. Everschor-Sitte, J. Masell, R. M. Reeve et al., J. Appl. Phys. 124(24), 240901 (2018).
7. A. S. Samardak, A. G. Kolesnikov, A. V. Davydenko et al., FMM 121, 260 (2022).
8. K. Raab, M. A. Brems, G. Beneke et al., Nat. Commun. 13, 6982 (2022).
9. D. Navas, R. V. Verba, A. Hierro-Rodriguez et al., APL Mater. 7, 0811114 (2019).
10. L. Liu, C.-T. Chen and J. Z. Sun, Nat. Phys. 10, 561 (2014).
11. F. Jonietz, S. Mühlbauer, C. Pfleiderer et al., Science 330, 1648 (2010).
12. A. Sparavigna, A. Strigazzi and A. Zvezdin, Phys. Rev. B. 50, 2953 (1994).
13. I. Dzyaloshinskii, Europhys. Lett. 83, 67001 (2008).
14. A. S. Logginov, G. A. Meshkov, A. V. Nikolaev et al., Appl. Phys. Lett. 93, 182510 (2008).
15. A. P. Pyatakov, A. K. Zvezdin, UFN 182, 593 (2012)
16. R. M. Vakhitov, Z. V. Gareeva, R. V. Solonetsky et al., FTT 61, 1120 (2019).
17. A. F. Kabychenkov, F. V. Lisovsky, E. G. Mansvetova, JETP Letters 97, 304 (2013).
18. G. V. Arzamastseva, A. M. Balbashov, F. V. Lisovsky et al., JETP 147, 793 (2015).
19. D. P. Kulikova, A. P. Pyatakov, E. P. Nikolaeva et al., JETP Letters 104, 196 (2016).

20. E. B. Magadeev and R. M. Vakhitov, J. Magn. Magn. Mater. 587, 171230 (2023).

21. E. B. Magadeev, R. M. Vakhitov, JETP Letters 115, 123 (2022).

22. E. B. Magadeev, R. M. Vakhitov, R. R. Kanbekov, JETP 162, 417 (2022).

23. E. B. Magadeev, R. M. Vakhitov, R. R. Kanbekov, JETP 163, 78 (2023).

24. K. L. Metlov, JETP Letters 118, 95 (2023).

25. E. Magadeev, R. Vakhitov, I. Sharafullin, Entropy 24, 1104 (2022).

26. P.I. Karpov and S.I. Mukhin, Phys. Rev. B 95, 195136 (2017).

27. A. Hubert and R. Shafer, Magnetic Domains, Springer-Verlag, Berlin (2007).

28. E. B. Magadeev, R. M. Vakhitov, and R. R. Kanbekov, Europhys. Lett. 142, 26001 (2023).